

System size dependence of nuclear modification and azimuthal anisotropy of jet quenching

Somnath De[‡] and Dinesh K. Srivastava[§]

Variable Energy Cyclotron Centre, 1/AF Bidhan Nagar, Kolkata-700 064, India

Abstract.

We investigate the system size dependence of jet-quenching by analyzing transverse momentum spectra of neutral pions in Au+Au and Cu+Cu collisions at $\sqrt{s_{NN}}=200$ GeV for different centralities. The fast partons are assumed to lose energy by radiating gluons as they traverse the plasma and undergo multiple collisions. The energy loss per collision, ε , is taken as proportional E (where E is the energy of the parton), proportional to \sqrt{E} , or a constant depending on whether the formation time of the gluon is less than the mean path, greater than the mean free path but less than the path length, or greater than the path length of the partons, respectively. NLO pQCD is used to evaluate pion production by modifying the fragmentation function to account for the energy loss. We reproduce the nuclear modification factor R_{AA} by treating ε as the only free parameter, depending on the centrality and the mechanism of energy loss. These values are seen to explain the nuclear modification of prompt photons, caused by the energy lost by final state quarks before they fragment into photons. These also reproduce the azimuthal asymmetry of transverse momentum distribution for pions within a factor of two and for prompt photons in a fair agreement with experimental data.

Keywords: Relativistic Heavy Ion Collisions, Quark gluon plasma, NLO pQCD, Jet quenching, Pion production, Direct photon production, Nuclear modification, Azimuthal anisotropy.

PACS No.: 12.38.Mh, 12.38.-t, 13.85.Qk, 25.75.Cj, 25.75.-q

[‡] somnathde@vecc.gov.in

[§] dinesh@vecc.gov.in

1. Introduction

Exploration of the properties of quark gluon plasma (QGP) produced in relativistic heavy ion collisions represents a major theme of modern nuclear physics research. The formation of QGP is heralded by numerous signatures, e.g., jet-quenching [1, 2], elliptic flow of hadrons [3, 4], quark number scaling of elliptic flow of hadrons[5], radiation of thermal photons [6, 7, 8, 9], and suppressed production of J/ψ [10, 11], etc. The celebrated phenomenon of jet-quenching has its origin in energy loss suffered by high energy quarks and gluons as they traverse the QGP, colliding with other partons and radiating gluons. It leads to a suppressed production of hadrons having large transverse momenta as compared to the case for NN collisions at the corresponding centre of mass energy per nucleon. It is measured in terms of the nuclear modification factor R_{AA} , given by:

$$R_{AA}(p_T, b) = \frac{d^2 N_{AA}(b)/dp_T dy}{T_{AA}(b)(d^2 \sigma_{NN}/dp_T dy)} \quad (1)$$

where b is the impact parameter and $T_{AA}(b)$ is the nuclear overlap function for impact parameter b .

The jet-quenching has several other manifestations. Thus, for example, in a non-central collision the jets moving in and out of the reaction plane would cover differing distances inside the plasma, lose differing amounts of energy, and would be quenched to a different extent. This will lead to an azimuthal anisotropy of momentum distribution of hadrons which does not have its origin in the so-called elliptic flow [12].

Next consider a high energy quark which is produced in a hard scattering. A photon fragmented off this quark contributes to the prompt photon production at high transverse momenta. The quark may lose energy before its fragmentation and thus this photon production may get suppressed [13, 14]. Following the same arguments as above, this may also lead to an azimuthal anisotropy in photon production for non-central collisions [15]. The jet-photon conversion [7] and jet-induced bremsstrahlung [8] lead to very small contributions with opposite signs for the azimuthal anisotropy of the photon productions [15] and are not considered in the present work.

A new dimension to the azimuthal asymmetry and the jet-quenching has been added by the realization that the event by event fluctuations of the initial conditions may affect the elliptic flow of the final state hadrons [16]. It is not very clear these seriously affect the azimuthal variation of the transverse momenta, which arises from jet-quenching [17] as well.

It is expected that the magnitude of all these effects will depend on the dynamics of the collision and the properties of the QGP. This makes jet-quenching a powerful probe of the QGP.

While there are quite a few detailed studies on the jet-quenching at RHIC and LHC energies [18], in the present work we continue the study reported in Ref. [13, 22], where the Wang, Huang, and Sarcevic model [23] was used to study the evolution of the mechanism of energy loss at RHIC and LHC energies in central collision of heavy

nuclei. The model treats the medium produced in the collision as a plasma of length L through which the partons move, undergoing multiple collisions, losing energy through radiated gluons, before fragmenting to form hadrons. The only parameters which then enter the calculations are the path-length- L , the mean-free path- λ , and the energy loss per collision- ε .

The energy loss per collision is then assumed to take a form as proportional to the energy of the parton- E , \sqrt{E} , or a constant; depending upon the formation time of the radiated gluons, which is less than the mean free path, larger than the mean free path but less than the path length L , and greater than the path length L , respectively. The three regimes are called the Bethe-Heitler regime, the LPM regime, and the complete coherence regime (as the entire medium radiates as a whole) [24]. The formation time (or length) of the radiated gluon is $\approx \omega/k_T^2$, where ω is the energy of the gluon and k_T is its transverse momentum.

In the present work we explore the limits of the above approach by performing a detailed and systematic study of medium modification of production of neutral pions and prompt photons having large transverse momenta as a function of centrality and system size, by analyzing the corresponding data at 200 GeV/nucleon for collisions of gold nuclei and copper nuclei. We first seek an accurate description of the medium modification parameter R_{AA} for different centralities and p_T , using the three approaches for the energy loss mechanisms, by varying the coefficients of energy loss, while accounting for the variation of the path length L . We find that the hadrons having low p_T (< 5 GeV/ c) fall into the Bethe-Heitler regime, those having intermediate p_T (5 GeV/ $c < p_T < 10$ GeV/ c) fall into the LPM regime, while those having large $p_T > 8$ – 10 GeV/ c are covered by the complete coherence regime. We find a systematic decrease of the energy loss per collision as we go to more peripheral collisions from central collisions, as one might expect.

We then use the same parameters to determine the azimuthal anisotropy coefficient $v_2(p_T)$ for neutral pions having large p_T . We find that in general, the experimentally obtained $v_2(p_T)$ is lower than those predicted by our calculations, though the trend is generally reproduced. Part of this discrepancy may have its origin in the uniform densities for the nuclei, used in the present work.

Next we calculate the prompt photon production as well as $v_2^{\gamma}(k_T)$. Again we get reasonable description of the experimental data. Further improvements can perhaps be made by relaxing the condition of equality of mean-free path and energy loss per collision for quarks and gluons assumed while obtaining a description for $R_{AA}^{\pi^0}$. This would, however, increase the number of parameters.

We give our formulation for particle production, multiple scattering, and energy loss as applied to pion production at $\mathcal{O}(\alpha_s^3)$ in Sec. 2. The centrality dependence of nuclear modification of neutral pions and parton energy loss (dE/dx) for Au-Au and Cu-Cu collisions at the highest RHIC energy are discussed in Sec. 3. The results for the azimuthal asymmetry of high p_T neutral pions are shown in Sec. 4. In Sec. 5, we give the results for the nuclear suppression and azimuthal anisotropy of prompt photons which

arise due to the modification of the fragmentation contribution. Finally we summarize our findings in Sec. 6.

2. Formulation

2.1. Particle production in pp collisions

In perturbative QCD, the inclusive cross-section for the production of a particle in proton-proton collisions is given by [25, 26]

$$\frac{d\sigma^{AB\rightarrow C}}{d^2p_T dy} = \sum_{a,b,c} \int dx_a \int dx_b \int \frac{dz}{z^2} F_{a/A}(x_a, Q^2) F_{b/B}(x_b, Q^2) D_{c/C}(z, Q_f^2) \frac{d\sigma_{ab\rightarrow c}}{d^2p_{cT} dy_c}, \quad (2)$$

where $F_{a/A}(x, Q^2)$ is the parton distribution function (PDF) for the parton a and $F_{b/B}(x, Q^2)$ is the PDF for the parton b , for the nucleons A and B respectively. $D_{c/C}$ gives the fragmentation probability of parton c into a particle C . In case of a hadron; $D_{c/h}$ is the fragmentation function evaluated at $z = p_h/p_c$, where z is the fraction of the parton's momentum carried by the hadron. In case of photon production, $D_{c/\gamma}$ gives the fragmentation probability of a photon fragmented off a quark with the momentum fraction $z = p_\gamma/p_c$. In addition, we have an extra term where photon is directly produced in the hard collision ($c = \gamma$). In that case the fragmentation function reduces to $\delta(1-z)$. $\sigma_{ab\rightarrow c}$ is the parton-parton cross-section, calculated for the leading order processes $\mathcal{O}(\alpha_s^2)$ such as:

$$\begin{aligned} q + q &\rightarrow q + q, \\ q + \bar{q} &\rightarrow q + \bar{q}, \\ q + g &\rightarrow q + g, \\ g + g &\rightarrow g + g, \\ \dots & \end{aligned} \quad (3)$$

At the next-to-leading order, $\mathcal{O}(\alpha_s^3)$ we include subprocesses like:

$$\begin{aligned} q + q &\rightarrow q + q + g, \\ q + \bar{q} &\rightarrow q + \bar{q} + g, \\ q + q' &\rightarrow q + q' + g, \\ q + \bar{q} &\rightarrow q' + \bar{q}' + g, \\ g + g &\rightarrow g + g + g \\ \dots & \end{aligned} \quad (4)$$

The running coupling constant $\alpha_s(\mu^2)$, is calculated at next-to-leading order

$$\alpha_s(\mu^2) = \frac{12\pi}{(33 - 2N_f) \ln(\mu^2/\Lambda^2)} \left(1 - \frac{6(153 - 19N_f) \ln \ln(\mu^2/\Lambda^2)}{(33 - 2N_f)^2 \ln(\mu^2/\Lambda^2)} \right), \quad (5)$$

where μ is the renormalization scale, N_f is the number of flavours, and Λ is the Λ_{QCD} scale. We have used the *CTEQ4M* structure function [27] and the BKK fragmentation function [28]. We set the factorization, renormalization, and fragmentation scales as equal to p_T , though we have checked scale dependence on particle production in pp collisions using $Q = 0.5p_T$ and $Q = 2.0p_T$ as well.

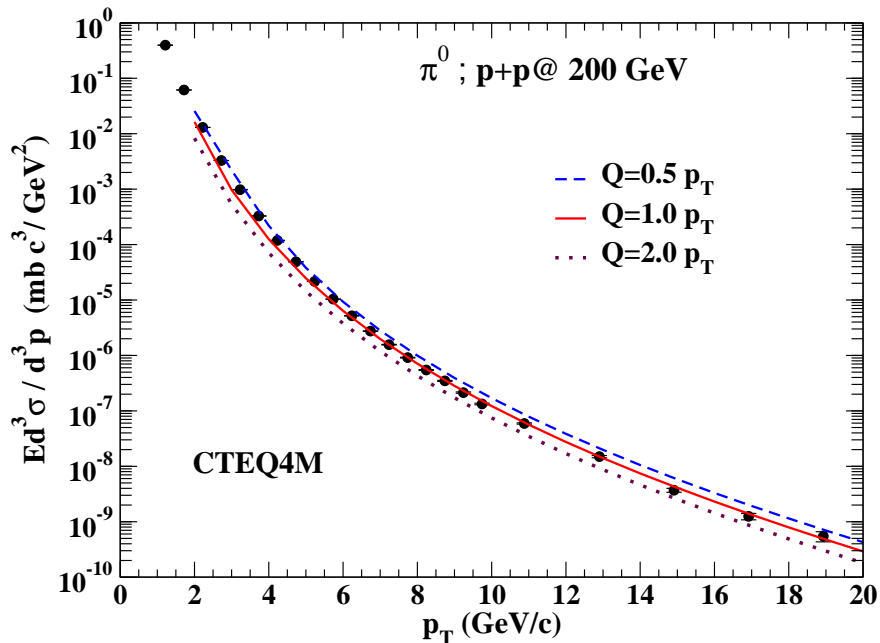


Figure 1. (Colour on-line) A comparison of neutral pion yield in p+p collision measured by the PHENIX collaboration [29] at $\sqrt{s_{\text{NN}}} = 200$ GeV with NLO pQCD calculations.

We show the results of our calculations for the inclusive neutral pion yield for proton-proton collisions at the centre of mass energy of 200 GeV along with the data from the PHENIX measurements [29] in Fig. 1. A very good agreement with the experimental data is seen, as in similar calculations by other authors (see e.g., Ref. [30]). The quantitative description of the data from pp collisions provides us with a reliable baseline to discuss nuclear modification of hadron production in nucleus-nucleus collisions.

2.2. Model for parton energy loss

In order to calculate the inclusive pion spectra from nucleus-nucleus collisions we have used the effects of shadowing and energy loss of partons. The nuclear shadowing accounts for the modification of the parton distribution function for nuclei compared to that for a free nucleon. The shadowing function is defined as:

$$S_{a/A}(x, Q^2) = \frac{F_{a/A}(x, Q^2)}{AF_{a/N}(x, Q^2)}, \quad (6)$$

where $F_{a/A}(x, Q^2)$ is the parton distribution for the nucleus A and $F_{a/N}(x, Q^2)$ is that for a nucleon. We have used the EKS98 parametrization of nuclear shadowing obtained

by Eskola, Kolhinen, and Salgado [31].

We use the simple phenomenological model, first used by Jeon et al. [13] to obtain a description of preliminary R_{AA} at RHIC energies, to estimate parton energy loss. The key features of this treatment are: average energy loss per collision (ε_a) by the parton, the mean free path of the parton (λ_a), and the average path length of the parton in the medium (L). The probability for a parton to scatter n times before leaving the medium can be written as:

$$P_a(n, L) = \frac{(L/\lambda_a)^n}{n!} e^{-L/\lambda_a}. \quad (7)$$

The multiple scattering and energy loss suffered by the partons then necessitates a modification of the fragmentation function $D_{c/h}(z, Q^2)$. Following the model of Wang, Huang, and Sarcevic [23], the modified fragmentation function can be written as:

$$zD_{c/h}(z, L, Q^2) = \frac{1}{C_N^a} \sum_{n=0}^N P_a(n, L) \times \left[z_n^a D_{c/h}^0(z_n^a, Q^2) + \sum_{m=1}^n z_m^a D_{g/h}^0(z_m^a, Q^2) \right] \quad (8)$$

where $zE_T^a = z_n^a E_n^a = z_n^a (E_T^a - \sum_{i=0}^n \varepsilon_a^i)$, $z_m^a = zE_T^a / \varepsilon_a^m$. N is the maximum number of collisions for which $z_n^a \leq 1$, $D_{c/h}^0$ is the hadronic fragmentation function which gives the probability that quark or gluon would fragment into a hadron (in our case π^0) and $C_N^a = \sum_{n=0}^N P_a(n, L)$. The first term gives the fragmentation probability of the leading parton a with a reduced energy ($E_T^a - \sum_{i=0}^n \varepsilon_a^i$) and the second term comes from the emitted gluon having energy ε_a^m .

While one may easily ignore the azimuthal (ϕ) dependence of the average path length $L(b)$ for impact parameter b for very central collisions, it needs to be considered for non-central collisions. We use a simple approach, based on Glauber model, to evaluate the dependence of the average path-length on the azimuthal angle with respect to the reaction plane. Assuming uniform densities for the colliding nuclei, the average path-length for an impact parameter b and azimuthal angle ϕ can be written as:

$$L(\phi; b) = \frac{\iint \ell(x, y, \phi, b) T_{AB}(x, y; b) dx dy}{\iint T_{AB}(x, y; b) dx dy}, \quad (9)$$

where x and y are the transverse co-ordinates for the point where the partons scatter to produce the jet(s) which, travelling at an angle ϕ with respect to the reaction plane, traverses the path length $\ell(x, y, \phi, b)$. $T_{AB}(x, y; b) = t_A(x + b/2, y)t_B(x - b/2, y)$ is the nuclear overlap function and t_A and t_B are the transverse density profiles of the two nuclei. An average of $L(\phi; b)$ over ϕ (varying from zero to 2π) gives the average path length $L(b)$ (see Fig. 2).

We closely follow the excellent review on jet-quenching by Baier et al [24], and assume that the collisional energy loss is quite small for light quarks and gluons

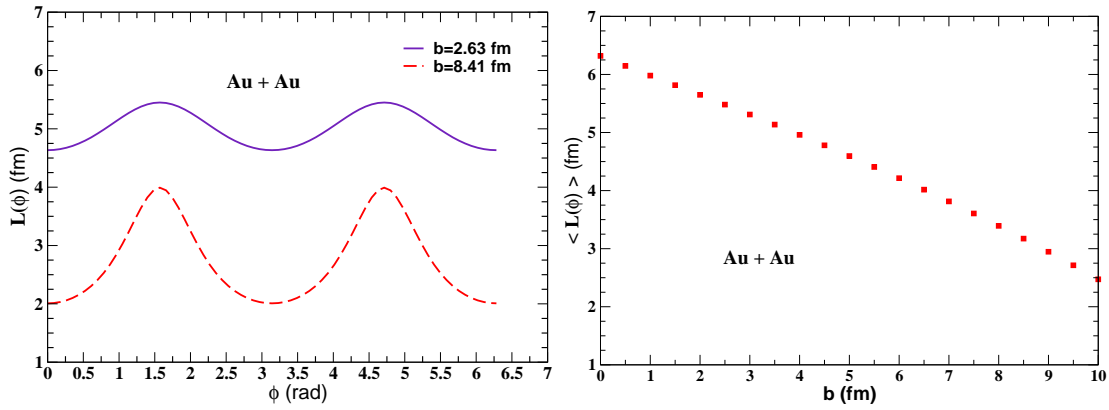


Figure 2. (Colour on-line) (Left panel) Azimuthal variation of the average path length traversed by a parton in collision of gold nuclei. The impact parameter for the upper curve is an average for 0-10% most central collisions and the lower one is for 40-50% centrality. (Right panel) The average path length vs. impact parameter for Au+Au system.

compared to the energy energy loss due to radiation of gluons. Now one can define the formation time of the radiated gluon as:

$$t_{\text{form}} \simeq \frac{\omega}{k_T^2} \quad (10)$$

where ω is the energy of the radiated gluon and k_T is the transverse momentum. We would normally have $\omega \gg k_T$ where $k_T \approx \mu$ is a typical momentum transfer in a partonic collision. The coherence length, l_{coh} , can now be written as:

$$l_{\text{coh}} \simeq \frac{\omega}{\langle k_T^2 \rangle_{\text{coh}}} \simeq \frac{\omega}{N_{\text{coh}} \langle k_T^2 \rangle}, \quad (11)$$

where N_{coh} is the number of coherent scattering centers. One can then write,

$$N_{\text{coh}} = \frac{l_{\text{coh}}}{\lambda_a} \simeq \sqrt{\frac{\omega}{\lambda_a \mu^2}} \equiv \sqrt{\frac{\omega}{E_{\text{LPM}}}} \quad (12)$$

where $E_{\text{LPM}} = \lambda_a \mu^2$ is the energy parameter introduced to separate the incoherent and coherent radiation of gluons.

In the Bethe-Heitler (BH) regime, the energy of the radiated gluon is less than E_{LPM} , the coherence length $l_{\text{coh}} \leq \lambda_a$, leading to an incoherent radiation from L/λ_a scattering centers. Thus energy loss per unit length in the soft ω limit becomes:

$$-\frac{dE}{dx} \approx \frac{\alpha_s}{\pi} N_c \frac{1}{\lambda_a} E, \quad (13)$$

where $N_c = 3$ and E is the energy of the parton. We shall write $\varepsilon_a \approx kE$ for this case and determine k from the measurement of R_{AA} .

For $\omega > E_{\text{LPM}}$, we have a regime of coherent radiation, where the coherence length l_{coh} is greater than λ_a but less than average path length L . Thus, $N_{\text{coh}} (> 1)$ centres of scattering radiate coherently leading to

$$-\frac{dE}{dx} \approx \frac{\alpha_s}{\pi} \frac{N_c}{\lambda_a} \sqrt{E_{\text{LPM}} E}. \quad (14)$$

We re-write this as $\varepsilon_a \approx \sqrt{\alpha E}$ and determine the values of α from the measurement of R_{AA} .

Finally, when the coherence length is larger than L ($l_{\text{coh}} > L$) the entire medium acts as one coherent source and energy loss per unit length becomes:

$$-\frac{dE}{dx} = \frac{\alpha_s}{\pi} N_c \frac{\langle k_T^2 \rangle}{\lambda_a} L . \quad (15)$$

This is denoted as constant energy loss ($\varepsilon_a = \kappa$) regime. We use the NLO code of Aurenche et al [25] adopted earlier by Jeon et al. [13] to account for the energy loss of the partons, by modifying the fragmentation function, for the calculations reported here.

A more detailed derivation of the energy loss for this case leads to:

$$-\frac{dE}{dx} = \frac{\alpha_s}{4} N_c \frac{\langle k_T^2 \rangle L}{\lambda_a} \tilde{v} . \quad (16)$$

where \tilde{v} is Fourier transform of the normalized differential cross-section for parton-parton collisions for the appropriate momentum transfer scale (see Ref. [24]). The momentum transport coefficient \hat{q} is then defined as:

$$\hat{q} = \frac{\langle k_T^2 \rangle}{\lambda_a} \tilde{v} , \quad (17)$$

so that we can write:

$$-\frac{dE}{dx} = \frac{\alpha_s}{4} N_c \hat{q} L , \quad (18)$$

which can be used to deduce the average momentum transport coefficient for any given centrality, for a comparison with other estimates for this.

3. Results

3.1. Centrality dependence of R_{AA} for Au-Au collisions at RHIC

We have calculated the nuclear modification factor R_{AA} for neutral pions for Au-Au collisions at the top RHIC energy for six centralities using Bethe-Heitler (BH), LPM, and constant energy loss mechanisms, discussed above. We have kept the mean free path of gluons as well as quarks fixed at 1 fm and also assumed that their energy loss per collision is identical. Thus once we have accounted for the variation of the average path length $L(b)$ with centrality, we are left with the energy loss per collision as the only adjustable parameter.

The results for BH mechanism are shown in Fig. 3 for near-central (0-10%, 10-20%, 20-30%) and mid-central (30-40%, 40-50%, 50-60%) collisions. We see a good description of the data for p_T up to about 6 GeV/ c . The necessary energy loss per collision is seen to slowly drop from 10% to about 8% of the energy of the partons as we move from near central to mid-central collisions. We also note that the slope of R_{AA} changes around p_T equal to 5 GeV/ c , which suggests a possible change in the mechanism for energy loss for partons contributing to higher momenta [22].

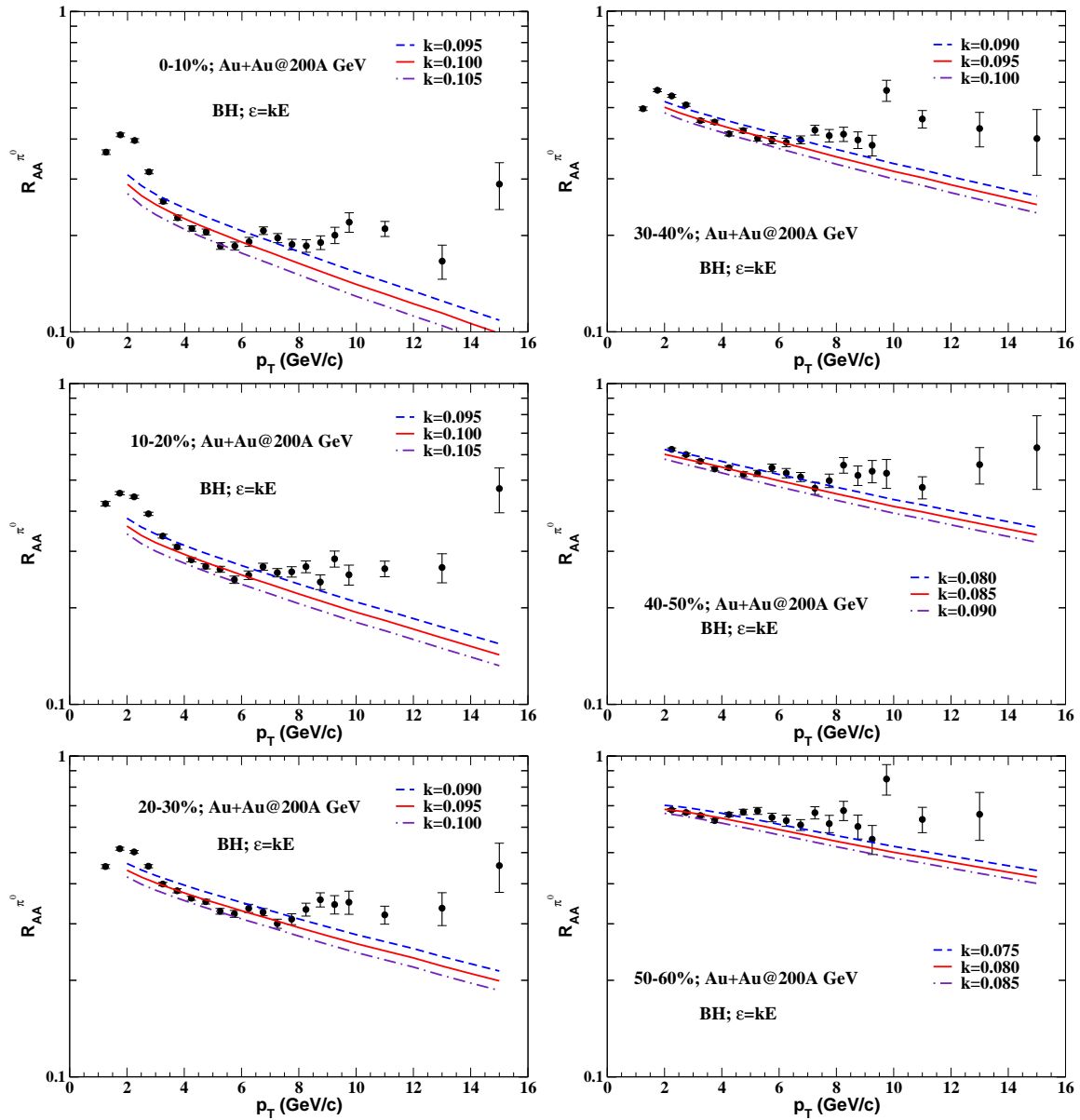


Figure 3. (Colour on-line) Nuclear modification of neutral pion production for Au+Au collisions at $\sqrt{s_{NN}}=200$ GeV, using BH mechanism (see text). The experimental data are taken from Ref. [32].

This expectation is confirmed by results shown in Fig. 4, where the so-called LPM mechanism of energy loss is seen to provide an accurate description of the nuclear modification function in the p_T range of 6–10 GeV/ c . Once again we note that the energy loss coefficient α decreases systematically as the collisions become less central. Thus a parton having an energy of 10 GeV is likely to lose about 1 GeV in the first collision in the most central collision considered here and about 0.7 GeV in the collisions having a centrality of about 50–60%.

Finally, we see (Fig. 5) that the medium modification function for hadrons having

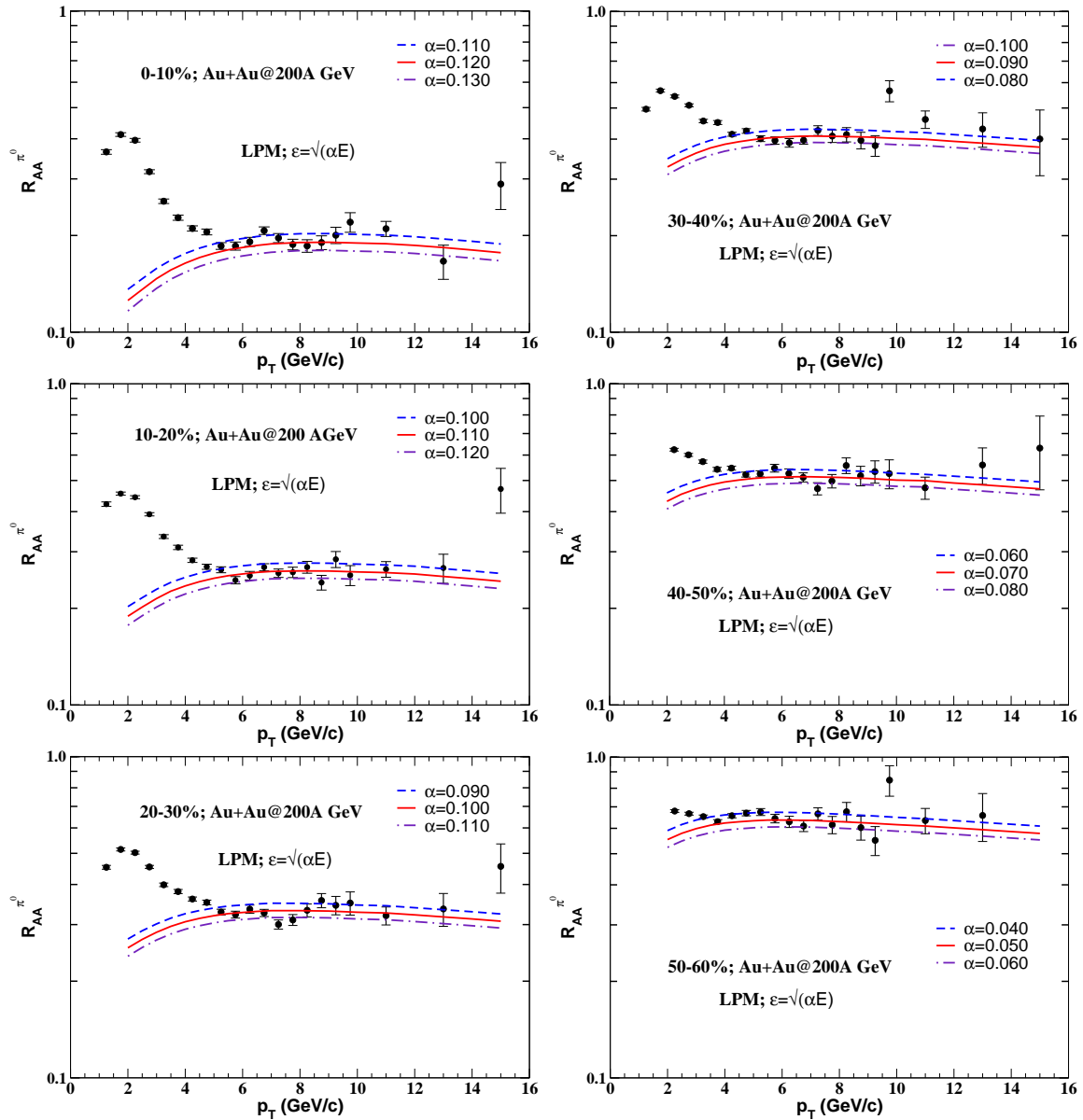


Figure 4. (Colour on-line) Nuclear modification of neutral pion production for Au+Au collisions at $\sqrt{s_{NN}}=200$ GeV using LPM mechanism. The experimental data are taken from Ref. [32].

$p_T > 8$ GeV/c is best described by the mechanism assuming a constant energy loss per collision. The energy loss per collision is seen to decrease from about 1.4 GeV for the most central collisions to about 1 GeV for the collisions having a centrality of 50–60%.

The transition from the BH regime to the LPM seen above and noted earlier [22] at $p_T \approx 5$ GeV/c should not come as a surprise to us, since for the mean free-path $\lambda \sim 1$ fm and $\langle k_T^2 \rangle \approx 1$ (GeV/c)² per collision, E_{LPM} is about 5 GeV, which roughly separates the BH and LPM energy loss regimes for all centralities

The results for these three figures are summarized in Fig. 6. Several interesting

facts emerge.

Let us first look at the results for the BH regime operating for p_T up to about 5–6 GeV/ c . We note as we go to more peripheral collisions the data, even for lower p_T , are in a better agreement with our calculations. This, we feel, is due to the reducing importance of radial flow (which gives a transverse kick to the partons/hadrons) in peripheral collisions.

The LPM regime operating over the p_T window of 5–10 GeV/ c and the complete coherence regime operating at higher p_T are seen to correctly describe the details of the changing curvature of the nuclear modification factor.

We add that a look at Fig. 4 may prompt one to conclude that the description using the LPM mechanism is also working reasonably well till the largest p_T considered here. However a closer look at the Figs. 4 and 5 reveal that the LPM description mostly misses the data for larger p_T values while the description using the constant energy loss per collision correctly reflects the curvature of the data till the largest p_T . A more accurate data extending up to even larger p_T would be very valuable to settle this question more firmly.

Even though we have identified the regions of the applicability of the mechanisms of energy loss, purely on the basis of a good description of the experimental values of the nuclear modification factor, it is heartening to note that the separation of the BH and the LPM regimes is very close to 5 GeV/ c expected by us, as discussed above. We recall that the LPM and the complete coherence regimes differ by the formation time of the gluons, which is larger than the mean free path but smaller than the path-length for the former, while it is larger than the path-length (and of-course the mean free path) for the later. This is reflected in a slight change in the curvature of the nuclear modification factor, around $p_T \approx 8$ –10 GeV/ c .

In brief, we have noted that the energy loss parameter in the Wang, Huang, and Sarcevic model for energy loss of partons in relativistic heavy ion collisions at RHIC can be tuned to obtain an accurate description of the nuclear modification factor R_{AA} for different ranges of the transverse momenta. This observation is further strengthened by Fig. 7 where the variation of R_{AA} integrated over p_T ranging from 6 to 9 GeV/ c is shown as a function of number of participants and compared with the data from PHENIX collaboration [33].

3.2. Centrality dependence of R_{AA} for Cu-Cu collisions at RHIC

In the next step we apply the above treatment to the collisions of copper nuclei at the same centre of mass energy of 200 GeV/nucleon. These collisions present an interesting system for the study of jet-quenching which complements as well as supplements the results from the collision of gold nuclei discussed earlier. It is well known that the more central collisions of copper nuclei have number of participants similar to those for mid-central collisions of gold nuclei. Thus a comparison would give us results for two systems, involving similar number of participants, one of which has nearly central

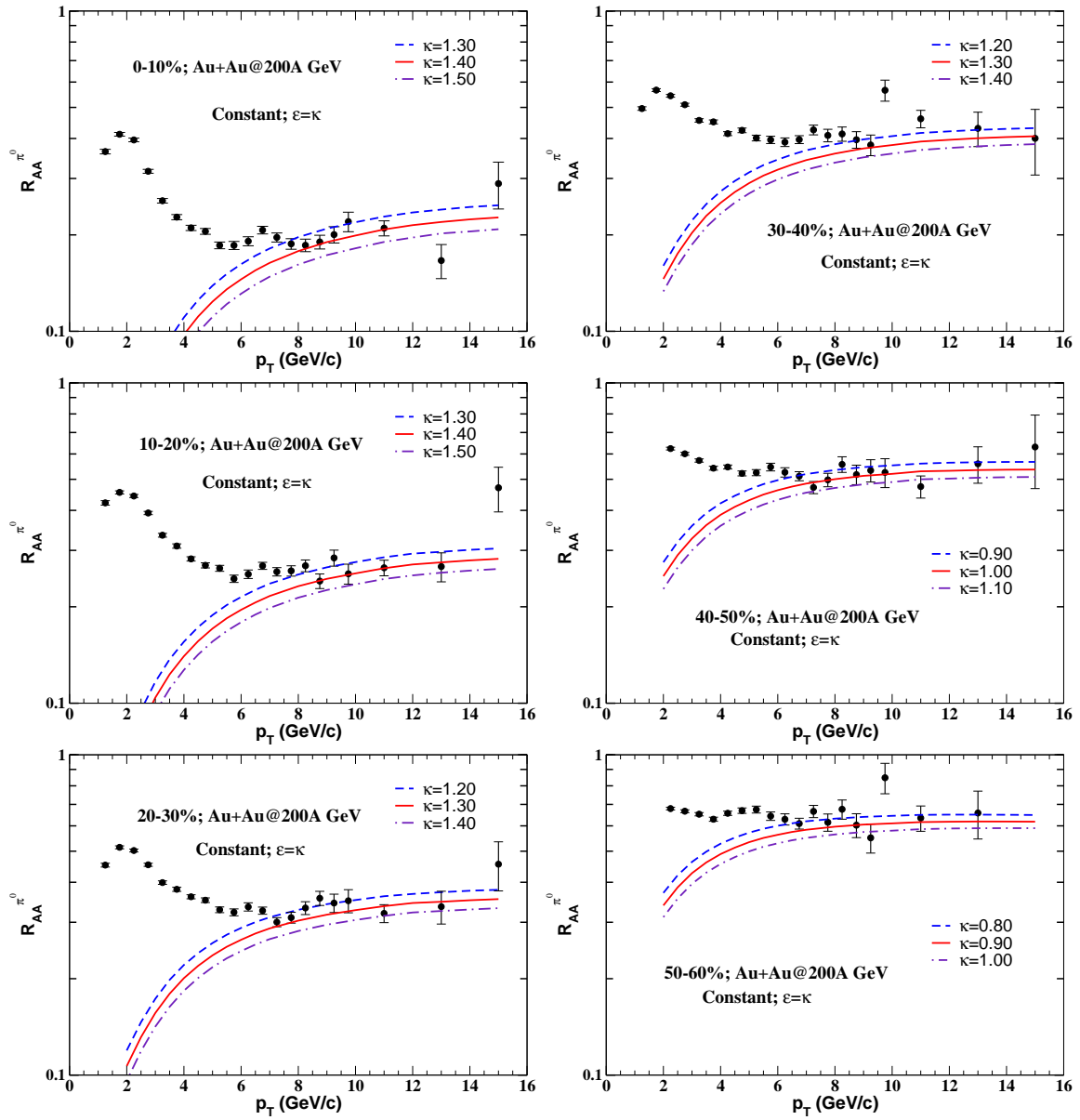


Figure 5. (Colour on-line) Nuclear modification of neutral pion production for Au+Au collisions at $\sqrt{s_{NN}}=200$ GeV assuming a constant energy loss/collision. The experimental data are taken from Ref. [32].

collisions and the other one has a large eccentricity.

Proceeding as before, we give our results for the nuclear modification factor R_{AA} for Cu+Cu collisions for centralities varying from 0–10% to 30–40%, in Figs. 8–10, using the BH, the LPM, and the constant energy loss mechanisms and compare with the measurements by PHENIX collaboration [34]. (See also Ref. [35]).

From Fig. 8, we see that the energy loss mechanism suitable for the BH regime provides an accurate explanation of the data for all the centralities under consideration for $p_T < 6$ GeV/ c .

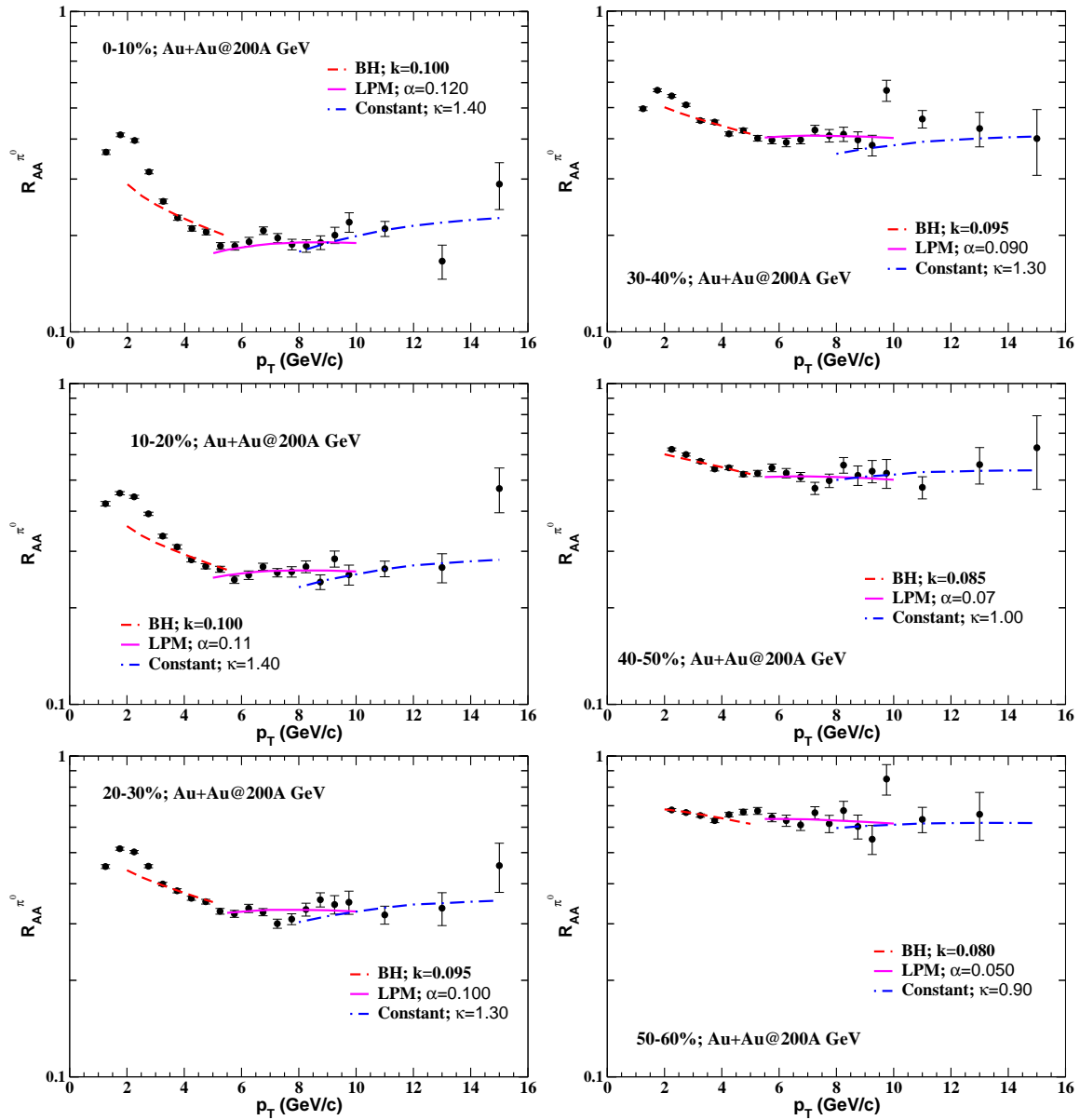


Figure 6. (Colour on-line) Nuclear modification of neutral pion production for Au+Au collisions at $\sqrt{s_{NN}}=200$ GeV for the three energy loss schemes for different p_T regimes.

The energy loss mechanism denoted as LPM is seen to describe the nuclear modification function over the p_T range of 6–10 GeV/ c and even beyond for less central collisions Fig. 9.

And finally, the results for the mechanism admitting a constant energy loss per collision is seen to work well for pions having $p_T >$ about 6–8 GeV/ c (see Fig. 10).

We note that the energy loss co-efficient for the most central collision of copper nuclei is close to that for the collision of gold nuclei for the 50–60% centrality, for all the three mechanisms. We also note the possible separation of the BH and LPM regimes around p_T equal to 5–6 GeV/ c , as before for gold collisions, though the demarcation of

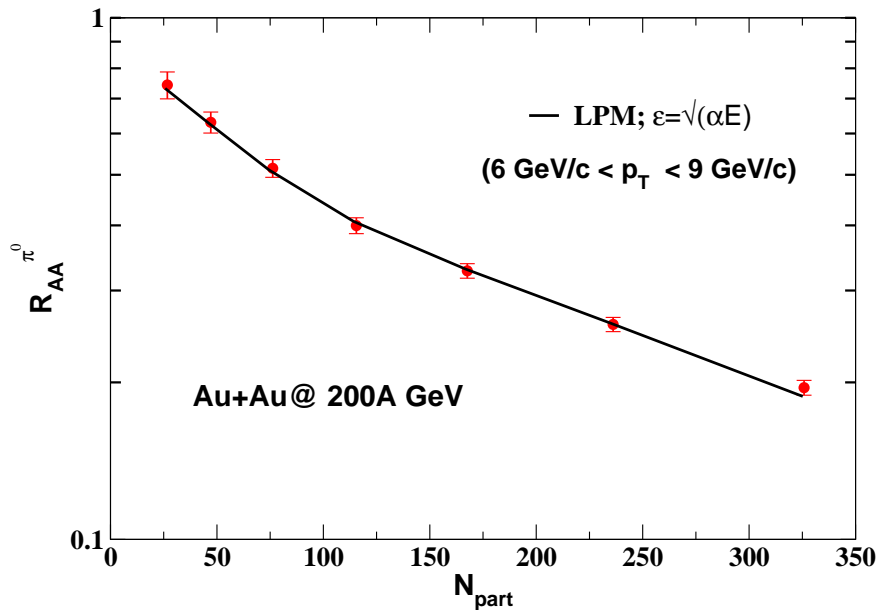


Figure 7. (Colour on-line) Centrality dependence of R_{AA} of neutral pions calculated for LPM mechanism of energy loss. The data are from the PHENIX collaboration [33] for Au+Au collisions at $\sqrt{s_{NN}} = 200$ GeV.

the LPM and the constant energy loss mechanisms is not as sharp for the copper nuclei as for the gold nuclei, especially for the less central collisions. This may have its origin in smaller L for copper nuclei.

A figure similar to Fig. 6 can also be prepared for the collisions involving copper nuclei. We have not given it here, for the want of space.

3.3. Centrality dependence of dE/dx

The results for the largest values of transverse momenta are summarized in Fig. 11. Taking the case of constant energy loss per collision, $-dE/dx = \varepsilon/\lambda$, we see that the rate of energy-loss necessary to explain the suppressed production of hadrons at large p_T varies as $\langle L \rangle$, the average path length of the partons in the medium, both for Cu+Cu and Au+Au collisions at the centre of mass energy of 200 GeV/nucleon. This empirical result confirms the conviction that for the range of transverse momenta covered, $p_T \geq 8-10$ GeV/ c , the concerned partons interact with the medium as a whole, and the energy lost by the partons, $\Delta E \propto L^2$. This is different from the AdS/CFT description where the radiated parton cloud is brought on-shell by the drag of the strongly coupled plasma and $\Delta E \propto L^3$ [36], though some moderation of the L dependence is expected for an expanding plasma.

We also see that even though the slopes of the results for Cu+Cu and Au+Au collisions are similar, the energy loss for a given $\langle L \rangle$ for Au+Au collisions is about 40–60% larger than that for Cu+Cu collisions.

We can use the Eq. 18 to obtain the value of the momentum transport coefficient,

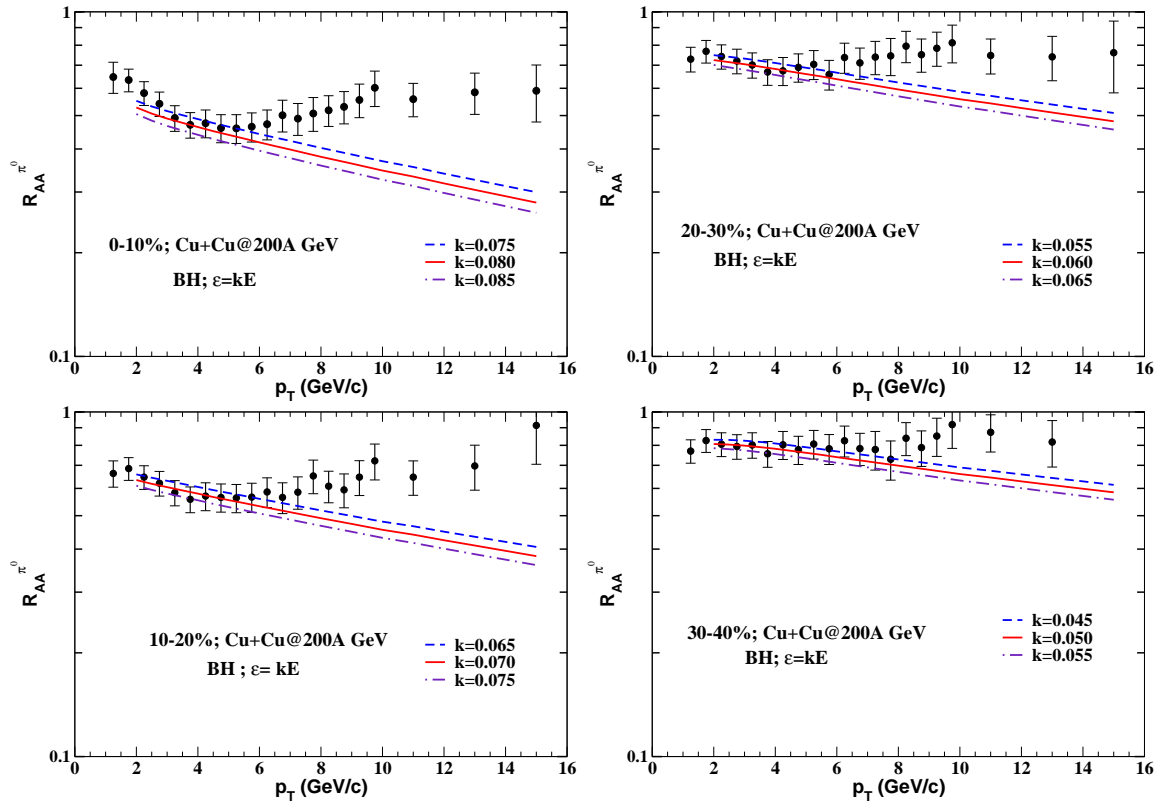


Figure 8. (Colour on-line) Nuclear modification of neutral pion production for Cu+Cu collisions at $\sqrt{s_{\text{NN}}}=200$ GeV for BH mechanism of energy loss along with the results from the PHENIX collaboration [34].

\hat{q} from the above. We find that the \hat{q} varies from $0.25 \text{ GeV}^2/\text{fm}$ for the collisions having 0–10% centrality for Au+Au system at 200 AGeV to $0.39 \text{ GeV}^2/\text{fm}$ for the 50–60% centrality. The decrease for more central collisions can be understood by noting that the systems produced in such cases would be at higher temperatures and thus much more dense than for peripheral collisions. This would then lead to a smaller suppression of the radiation due to the LPM effect. The faster rise with the path-length (L^2) more than compensates this decrease, finally giving a large energy loss and larger suppression of high momentum particles for more central collisions.

On the other hand, for the case of Cu+Cu system, we get $\hat{q} \approx 0.18 \text{ GeV}^2/\text{fm}$ for all the centralities considered by us. We note that it is about half of what we got for Au+Au system. The near identity of \hat{q} for all the centralities for Cu+Cu system is related to a smaller variation in the path-length for them. We also note that the Au+Au system is more efficient in degrading the jet-energy.

We add that various authors have reported widely differing values of \hat{q} . Thus, Wiedemann and Salgado [18] have reported a value of $5\text{--}10 \text{ GeV}^2/\text{fm}$, while Gyulassy, Levai, and Vitev [18] report a value in the range of $0.35\text{--}0.85 \text{ GeV}^2/\text{fm}$. Arnold, Moore, and Yaffe [18], on the other hand, suggest a value of about $2 \text{ GeV}^2/\text{fm}$, in contrast to a value of $3\text{--}4 \text{ GeV}^2/\text{fm}$ reported by Majumder [19, 20, 21]. It is felt that a part of this

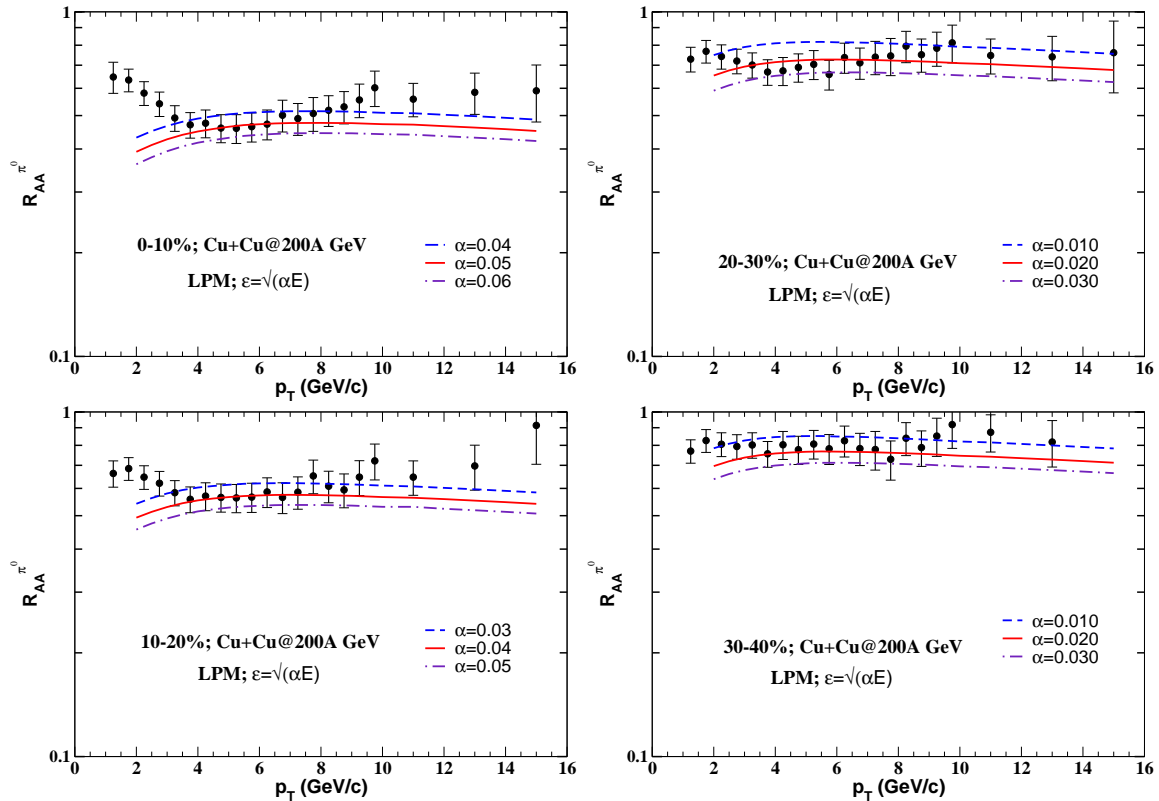


Figure 9. (Colour on-line) Nuclear modification of neutral pion production for Cu+Cu collisions at $\sqrt{s_{\text{NN}}}=200$ GeV for LPM mechanism of energy loss and compared with PHENIX results [34].

difference may be due to different physical attributes of the evolving system over which the average is taken.

4. Azimuthal anisotropy of high p_T neutral pions

We have seen that the phenomenological model of parton energy loss, which accounts for only the induced gluon radiation of the fast partons, successfully describes the suppression of neutral pion spectra at large p_T at different centralities for Au+Au and Cu+Cu collisions at $\sqrt{s_{\text{NN}}} = 200$ GeV. In case of non-central collisions, the path-length will have an azimuthal variation over the transverse plane (see Fig. 2). In what follows, we study the azimuthal dependence of the suppression of production of hadrons in terms of the azimuthal anisotropy of their transverse momenta [12].

We re-emphasize that this anisotropy is different from the elliptic flow seen for hadrons at lower p_T , which is explained using hydrodynamics which converts the spatial anisotropy of the initial state into the azimuthal anisotropy of the transverse momenta of the hadrons [3]. The extent of validity of hydrodynamics for larger p_T is not very clear. The success of the recombination model [5] suggests that the fragmentation as a mode of hadronization may be valid for $p_T \gg 3\text{--}5$ GeV/ c . Thus the following results

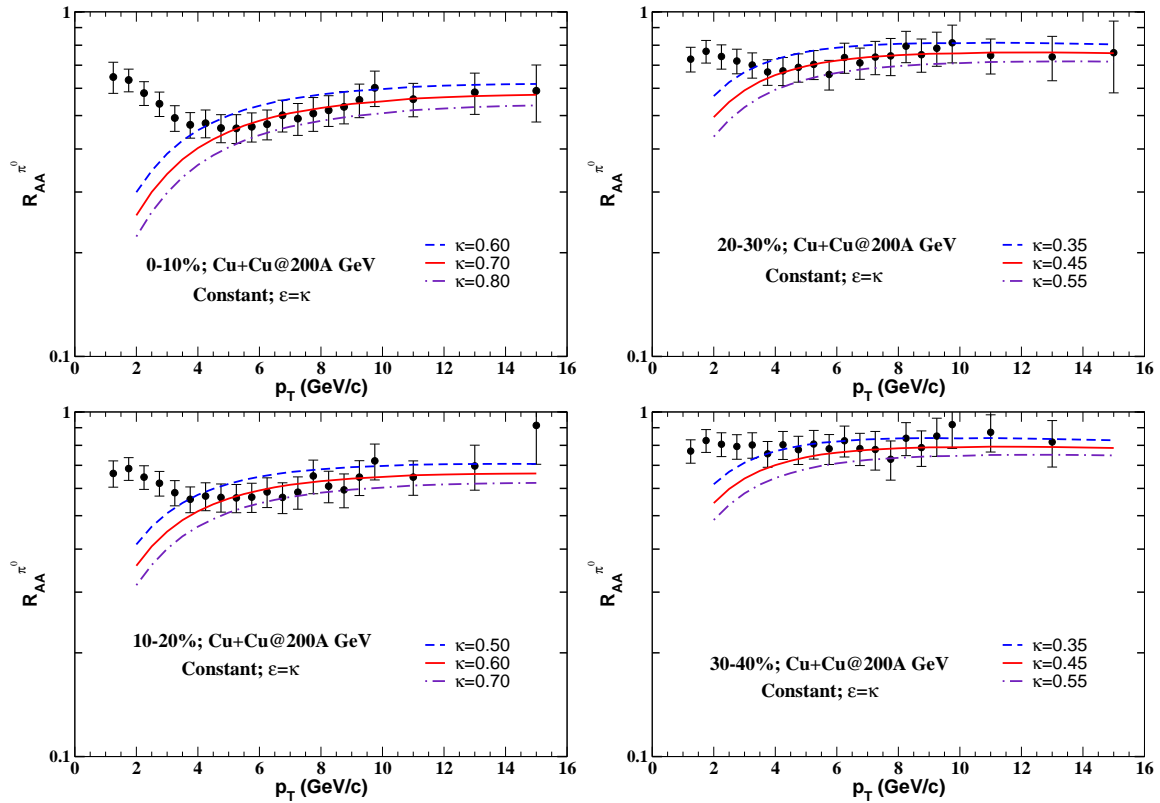


Figure 10. (Colour on-line) Nuclear modification of neutral pion production for Cu+Cu collisions at $\sqrt{s_{NN}}=200$ GeV for constant energy loss mechanism compared with PHENIX results [34].

should be taken as indicative of anisotropy which can arise due to medium modification of fragmentation function due to energy loss of partons.

The differential azimuthal anisotropy is measured in terms of the parameter $v_2(p_T)$, which is the second Fourier coefficient of the azimuthal distribution of hadrons in the reaction plane:

$$v_2(p_T) = \frac{\int_0^{2\pi} d\phi \cos(2\phi) dN/d^2p_T dy}{\int_0^{2\pi} d\phi dN/d^2p_T dy}. \quad (19)$$

We have calculated the azimuthal anisotropy coefficient $v_2(p_T)$ of neutral pions for $p_T > 2$ GeV/c for Au+Au collisions at $\sqrt{s_{NN}}=200$ GeV for the six centralities mentioned earlier. The energy loss per collision is taken from the earlier analysis and ϕ dependent distribution of the pions is calculated by incorporating the ϕ dependence of the path-length L .

The results of our calculations are displayed in Fig. 12 along with the data available from PHENIX collaboration [33]. We show the theoretical results only over the p_T window where the corresponding mechanism was found to describe the nuclear modification data, earlier (see Fig. 6).

Recalling that the BH mechanism was found to provide a good description of the nuclear suppression, up to p_T equal to 5–6 GeV/c, while the mechanisms for the LPM

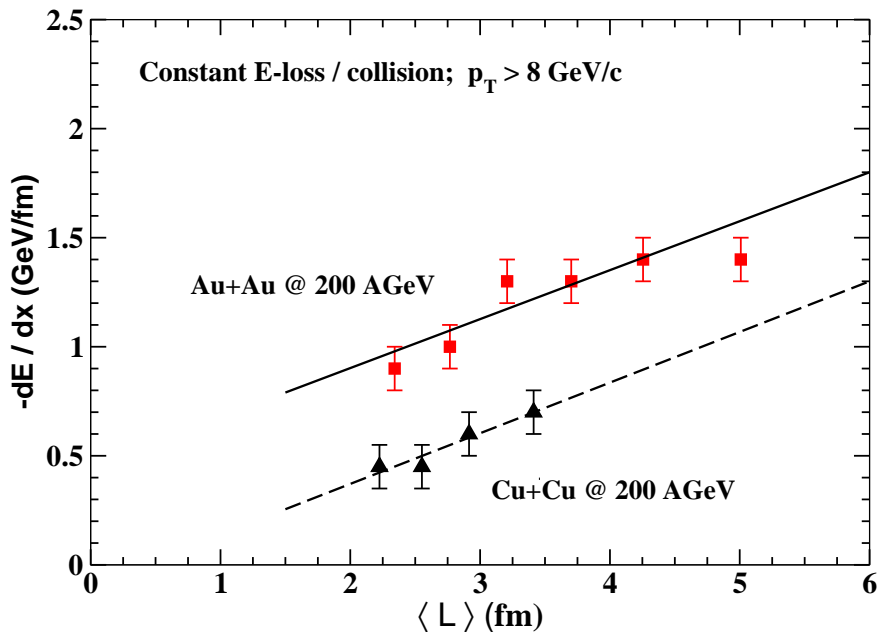


Figure 11. (Colour on-line) Variation of dE/dx with $\langle L \rangle$ for Cu+Cu and Au+Au collisions at 200 AGeV for the constant energy loss per collision regime obtained in the present work.

and the constant energy loss per collision provided description for higher p_T , the results are quite interesting. First of all, even for $p_T \leq 6$ GeV/ c while the BH mechanism leads to a $v_2(p_T)$ increasing with p_T , the experimental results show a contrary behaviour. It could be that a hydrodynamic expansion of the system under viscosity affects the hadrons having p_T up to 5–6 GeV/ c [37]. The other two mechanisms, though, give a behaviour similar to the experimental data, in the region of transverse momenta where they are applicable. The theoretical values are larger by up to a factor of two in the worst cases of more central collisions, though they agree reasonably well with the experimental values for the least central collision considered here.

It is interesting to see the centrality dependence of the integrated azimuthal anisotropy coefficient in the p_T range of 6–9 GeV/ c . For this purpose, we have used the differential azimuthal anisotropy coefficient $v_2(p_T)$ for the LPM mechanism obtained earlier (see Fig.13). We see that in general our calculations reproduce the trend of the variation of v_2 with the number of participants, though the theoretical values are larger by about a factor of two (see Ref. [38], for similar results). One short-coming of our calculation immediately comes to mind- the description of the nuclei as having a uniform density. A Woods-Saxon density profile for the colliding nuclei would reduce the difference in the path-lengths for the partons travelling in the reaction plane and travelling in a plane perpendicular to it, for example, and thus reduce v_2 . We postpone this study to a future work where additionally, the evolution of the medium will be taken into account.

We also give our prediction for $v_2(p_T)$ for Cu+Cu collisions at 200A GeV for two

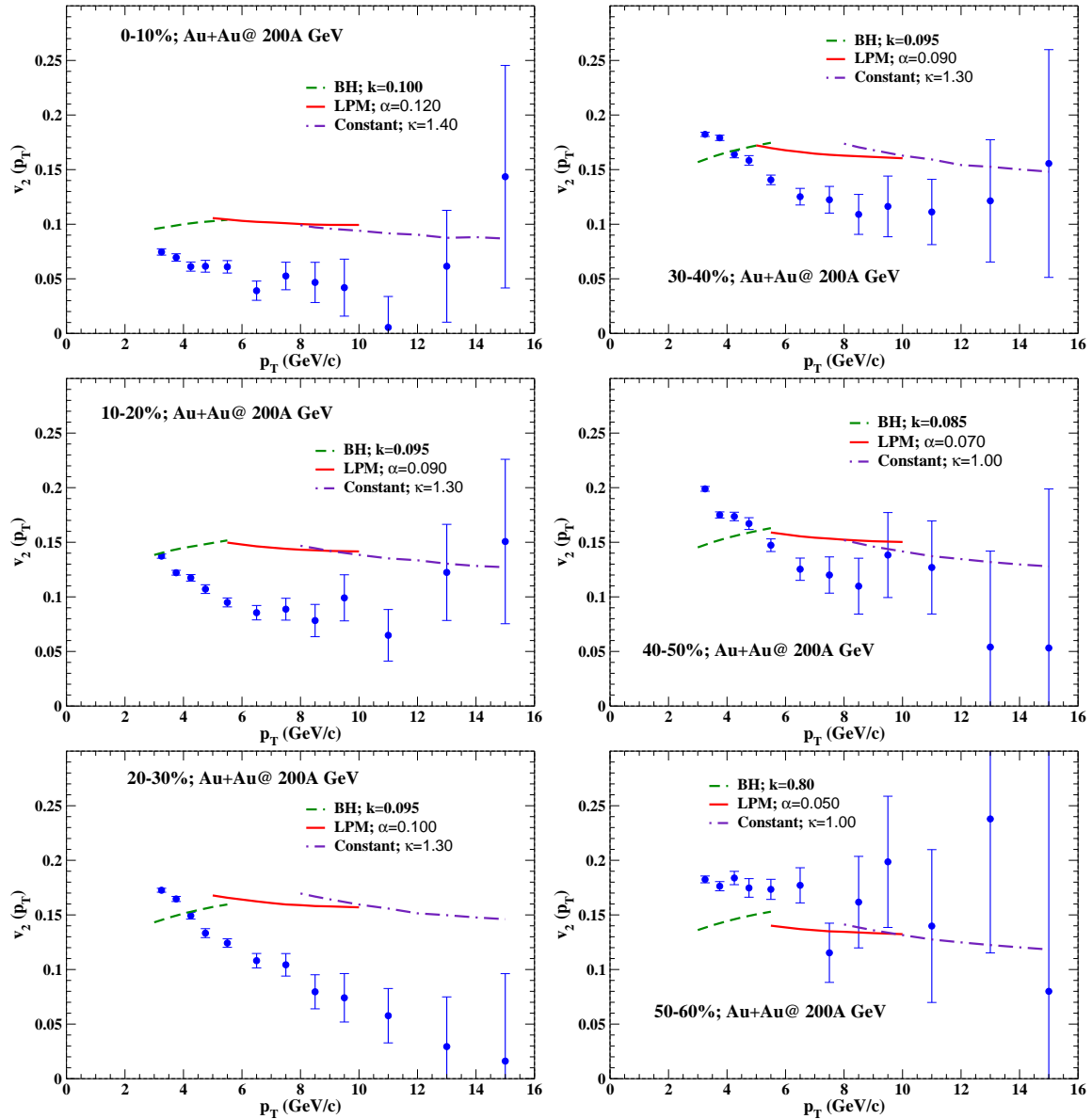


Figure 12. (Colour on-line) The differential azimuthal anisotropy coefficient v_2 of neutral pion calculated using BH, LPM, and constant energy loss mechanisms for Au+Au collisions at $\sqrt{s_{NN}}=200$ GeV. The experimental data are from the PHENIX collaboration [33].

typical centralities (Fig. 14). A behaviour similar to that for Au+Au collisions is seen.

5. Nuclear suppression and azimuthal asymmetry of prompt photons

Prompt photons, as indicated earlier, originate from (a) quark-gluon Compton scattering ($q + g \rightarrow q + \gamma$), (b) quark-anti-quark annihilation ($q + \bar{q} \rightarrow g + \gamma$), and (c) collinear fragmentation of a high energy quarks ($q \rightarrow q + \gamma$) following a hard collision. Of these the third process is affected by the energy loss suffered by the quark before its

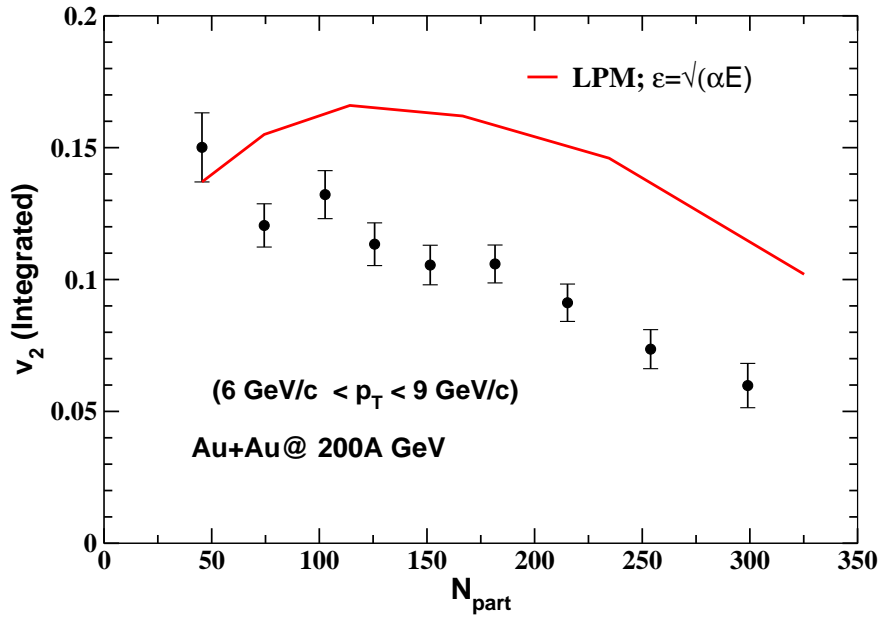


Figure 13. (Colour on-line) The centrality dependence of integrated v_2 of neutral pions calculated for LPM mechanism of energy loss for Au+Au collisions $\sqrt{s_{NN}} = 200$ GeV. The data points are taken from PHENIX collaboration [33].

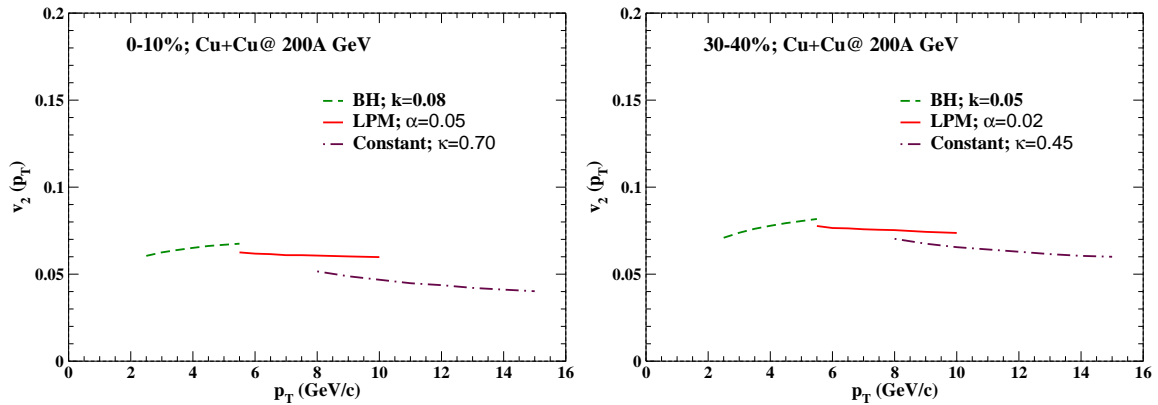


Figure 14. (Colour on-line) The differential azimuthal anisotropy coefficient $v_2(p_T)$ of neutral pion calculated using BH, LPM, and constant energy loss mechanisms for Cu+Cu collisions at $\sqrt{s_{NN}}=200$ GeV.

fragmentation [13, 14]. It will also lead to an azimuthal anisotropy of the momentum distribution of hard photons [15].

Once again, we use the NLO pQCD code of Aurenche et al [26], suitably modified to account for the energy loss suffered by the quarks before they fragment into photons. As a first step we show our results for proton-proton collisions at 200 GeV (Fig. 15) using the fragmentation, factorization, and the renormalization scales as equal, with $Q = k_T/2$, k_T and $2k_T$. We have used the *CTEQ4M* parton distribution function and the BKK fragmentation function for these calculations as well. We see that our results

are consistent with the data from PHENIX [39] and also with earlier calculations (see Ref. [39]) along similar lines. For the rest of the calculations we have used a common scale $Q = k_T$.

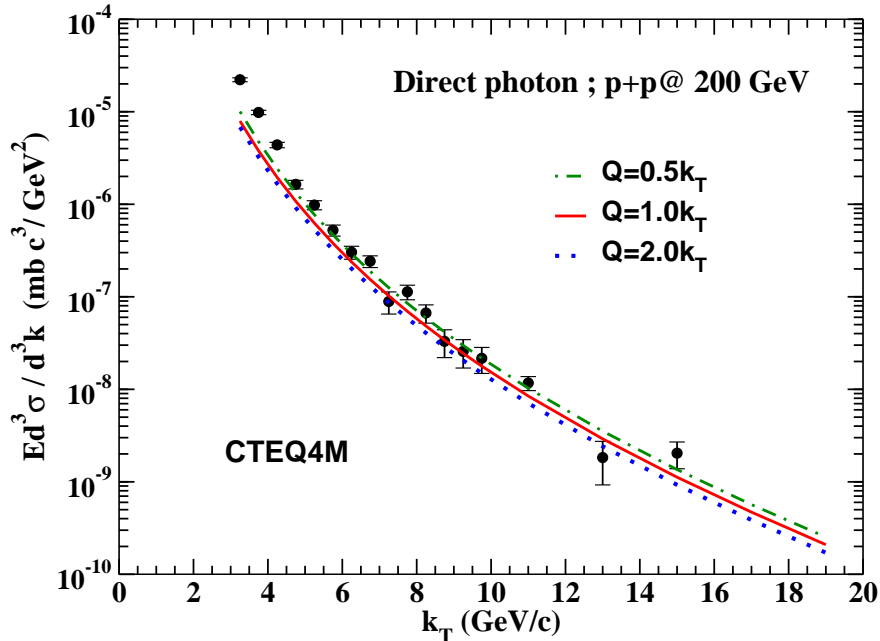


Figure 15. (Colour on-line) A comparison of production of prompt photons in p+p collision measured by the PHENIX collaboration [39] at $\sqrt{s_{NN}} = 200$ GeV with NLO pQCD calculations.

While performing the calculations for the nucleus-nucleus collisions we include nuclear shadowing and energy loss suffered by the quarks as before. We also properly account for the isospin of the participating nucleons, which is essential while performing calculations for photons. The nuclear modification factor R_{AA}^γ is then obtained in a manner similar to Eq. 1.

We show our results for the nuclear modification of hard photon production using the energy loss parameters obtained earlier along with the experimental results for collision of gold nuclei at 200A GeV in Fig. 16. We give the theoretical curves over the regions where the nuclear modification for pion production is in agreement with the experimental data (see Fig. 6).

We see that our results are in fair agreement with the data for k_T beyond 10 GeV/c where the mechanism of prompt photon production included in the present work is expected to dominate [14]. We do realize that for lower k_T other mechanisms like jet-conversion [7], induced bremsstrahlung [8] and thermal production [9] will contribute.

Next we calculate the the differential azimuthal anisotropy coefficient $v_2^\gamma(k_T)$ for hard photons for Au+Au collisions at 200A GeV. Recall that for lower k_T ($\leq 5-6$ GeV/c), the azimuthal anisotropy of the direct photons carries valuable information about the development of the elliptic flow of the plasma and momentum anisotropy of

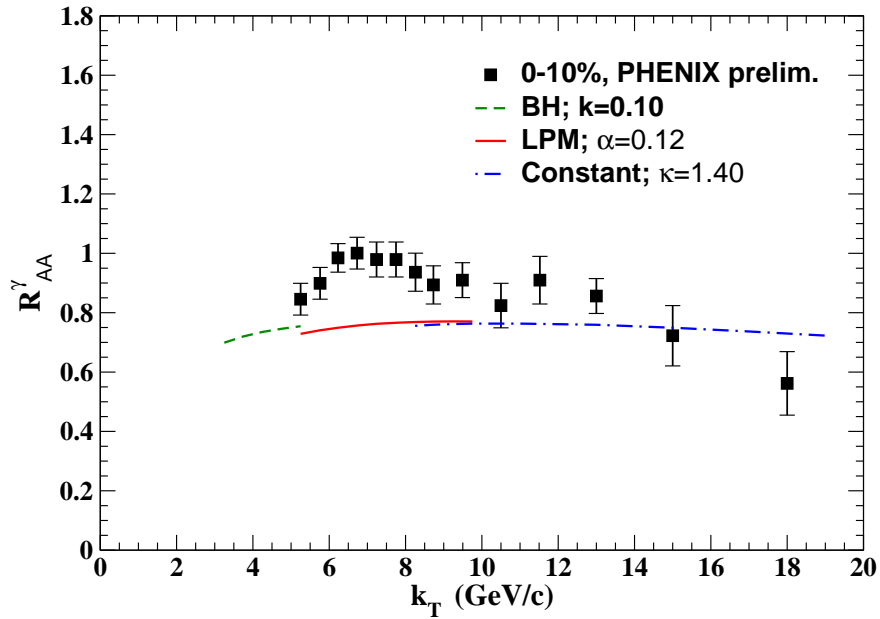


Figure 16. (Colour on-line) Nuclear suppression of hard photons calculated using BH, LPM, and constant energy loss per collision for Au+Au (0-10%) collisions at $\sqrt{s_{NN}}=200$ GeV. The data points are taken from Ref. [40]

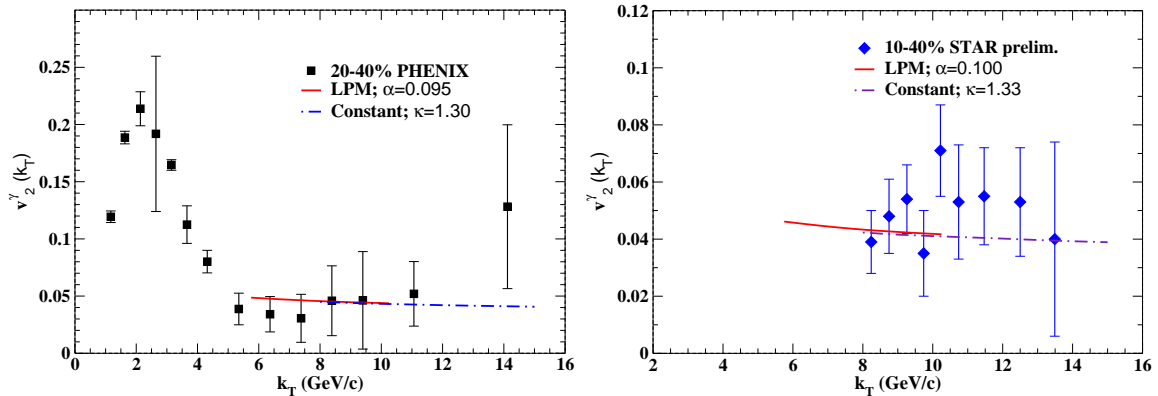


Figure 17. (Colour on-line) The differential azimuthal anisotropy coefficient v_2^γ of direct photons calculated using LPM scheme of parton energy loss for Au+Au collisions at $\sqrt{s_{NN}}=200$ GeV along with experimental results from the PHENIX [42] (left panel) and the STAR [43] (right panel) collaborations.

the thermalized partons [41].

In Fig. 17 we have shown the results for $v_2^\gamma(k_T)$ calculated using LPM and the constant energy loss per collision mechanisms of parton energy loss for two centrality classes (20-40% and 10-40%) and compared them with the recent results from the PHENIX [42] and the STAR [43] collaborations. We make no further adjustments of the energy loss parameters obtained earlier.

We see that the azimuthal anisotropy of direct photons for $k_T > 6$ GeV/c is

reproduced reasonably well from our calculations. The results of Figs. 16 and 17 come a pleasant surprise as we recall that while calculating the energy loss of the partons and the consequent suppression of hadrons at large p_T , we did not distinguish between quarks and gluons. The photon production, however, is sensitive only to the energy loss suffered by quarks. One possible reason for this could be the dominating contribution of quarks to hadrons as well photons having large transverse momenta, which is then rightly sampled by our procedure. One could use this procedure to first fix the energy loss per collision for quarks and then proceed to determine the energy loss per collision for gluons by fitting the hadronic spectra. This would, however, require a much more accurate and extensive large transverse momentum data for photons. A further availability of isolated photon spectra along with the (total) single photon spectra will help us to subtract out the Compton plus annihilation contributions and increase the sensitivity of these calculations to energy loss suffered by quarks.

6. Summary and Discussion

We have used a simple and transparent model of multiple scattering and energy loss for partons passing through quark gluon plasma produced in relativistic collisions of heavy nuclei, before they fragment into hadrons or photons. Taking the centrality dependence of the average path-length into account and taking energy loss per collision as an adjustable parameter, we have obtained a description of hadronic suppression in Au+Au and Cu+Cu collisions at 200A GeV. The energy loss parameters are found to vary systematically with the centrality and the dE/dx for $p_T > 6-8$ GeV/ c is found to vary linearly with the average path-length $\langle L \rangle$, in agreement with the predictions of Baier et al. [24].

The same parameters are then used without any further adjustments to obtain the azimuthal anisotropy for high p_T pions. We find it to be about a factor of two larger than the experimental values. Next, we have calculated the suppressed production of hard photons and their azimuthal anisotropy, again without changing any of the parameters. These are in reasonable agreement with the experimental findings. We have mentioned that in principal, the calculations could be improved by incorporating diffused density distributions for the colliding nuclei, instead of the uniform densities used in the present work. In that case, it remains to be seen if the v_2 could be used to further constrain the energy loss parameters.

The success of the approach, considering that the dynamics of evolution, the temperature and flavour dependence of some of the parameters and a more detailed accounting of various interferences are not considered here, once again confirms the inadequacy of R_{AA} in seriously distinguishing various details of the dynamics of the plasma [21].

Some improvements are definitely in order. The use of uniform density for the colliding nuclei can be easily improved upon. This, as we argued, could improve the description of azimuthal anisotropy of hadron production at higher p_T . One may also

take differing values for the mean free paths for quarks and gluons and the energy loss per collision for them. Note, however, that if we argue that dE/dx for gluons is twice that for quarks and also that their mean free path is half of that for quarks, then the energy loss for quarks and gluons per collision will be identical.

Why does this simple approach work so well? We realize that the p_T distribution of jets produced in primary hard scatterings is a rapidly falling function of the transverse momentum. Partons having a transverse momentum p_T after undergoing multiple collisions and losing a momentum Δp_T will populate the momentum space occupied by partons having transverse momentum $p_T - \Delta p_T$ while the later will shift to still lower momenta. Thus if we make a good estimate of Δp_T , we are likely to get a good description of the nuclear modification.

But is this approach really so simple? NLO pQCD and accurate structure and fragmentation functions, along with the applicability of pQCD at larger transverse momenta ensure an accurate base-line for p+p collisions. The influence of the dynamics of evolution is perhaps softened by the short life-time of the plasma at RHIC energies and the fact that most of the energy is lost in collisions at early times.

Thus we feel that the present study, at the very minimum, gives a reliable average of the rate of energy loss of partons in quark gluon plasma. We also see that a simultaneous description of nuclear modification of photon and pion production in nuclear collisions, holds out the hope of getting the energy loss suffered by quarks and gluons independently.

It will definitely be of interest to see if the centrality dependence of dE/dx ($\propto \langle L \rangle$) for partons having larger transverse momenta at LHC energies (2.76 ATeV and 5.5 ATeV) continues to follow the trend seen for the data at RHIC energies for Cu+Cu and Au+Au collisions, seen in Fig. 11. If confirmed at LHC energies as well, this will be a very valuable empirical affirmation of the suggestions of Baier et al [24]. This aspect is under investigation.

Acknowledgments

SD would like to express his sincere gratitude to Department of Atomic Energy, Government of India for financial support during the course of this work. We also thank Christine Aidala for drawing our attention to the final data for pp collisions (Fig. 1).

References

- [1] M. Gyulassy and M. Plümer, Phys. Lett. B **243**, 432 (1990);
X. N. Wang and M. Gyulassy, Phys. Rev. Lett. **68**, 1480 (1992);
M. Gyulassy, M. Plümer, M. Thoma and X. N. Wang, Nucl. Phys. A **538**, 37C (1992).
- [2] K. Adcox *et al.* [PHENIX Collaboration], Phys. Rev. Lett. **88**, 022301 (2002); J. Adams *et al.* [STAR Collaboration], Phys. Rev. Lett. **91**, 172302 (2003).
- [3] J. Y. Ollitrault, Phys. Rev. D **46**, 229 (1992);

- P. Huovinen, P. F. Kolb, U. W. Heinz, P. V. Ruuskanen and S. A. Voloshin, Phys. Lett. B **503**, 58 (2001);
D. Teaney, J. Lauret and E. V. Shuryak, [arXiv:nucl-th/0110037].
- [4] S. S. Adler *et al.* [PHENIX Collaboration], Phys. Rev. Lett. **91**, 182301 (2003); C. Adler *et al.* [STAR Collaboration], Phys. Rev. Lett. **87**, 182301 (2001).
- [5] R. J. Fries, B. Müller, C. Nonaka and S. A. Bass, Phys. Rev. Lett. **90**, 202303 (2003); R. J. Fries, B. Müller, C. Nonaka and S. A. Bass, Phys. Rev. C **68**, 044902 (2003); V. Greco, C. M. Ko and P. Levai, Phys. Rev. Lett. **90**, 202302 (2003).
- [6] A. Adare *et al.* [PHENIX Collaboration], Phys. Rev. Lett. **104** (2010) 132301;
S. S. Adler *et al.* [PHENIX Collaboration], Phys. Rev. Lett. **94**, 232301 (2005).
- [7] R. J. Fries, B. Müller and D. K. Srivastava, Phys. Rev. C **72**, 041902 (R) (2005); R. J. Fries, B. Müller and D. K. Srivastava, Phys. Rev. Lett. **90**, 132301 (2003).
- [8] B. G. Zakharov, JETP Lett. **80**, 1 (2004), [hep-ph/0405101].
- [9] S. A. Bass, B. Müller and D. K. Srivastava, Phys. Rev. Lett. **90**, 082301 (2003);
S. Turbide, C. Gale, S. Jeon and G. D. Moore, Phys. Rev. C **72**, 014906 (2005);
P. B. Arnold, G. D. Moore, L. G. Yaffe, JHEP **0112**, 009 (2001);
S. Turbide, R. Rapp and C. Gale, Phys. Rev. C **69**, 014903 (2004);
J. e. Alam, J. Phys. G **34**, S865 (2007);
D. G. d'Enterria and D. Peressounko, Eur. Phys. J. C **46**, 451 (2006).
- [10] T. Matsui and H. Satz, Phys. Lett. B **178**, 416 (1986); R. L. Thews, M. Schroedter and J. Rafelski, Phys. Rev. C **63**, 054905 (2001); X. M. Xu, D. Kharzeev, H. Satz and X. N. Wang, Phys. Rev. C **53**, 3051 (1996); B. K. Patra and D. K. Srivastava, Phys. Lett. B **505**, 113 (2001); L. Yan, P. Zhuang and N. Xu, Phys. Rev. Lett. **97**, 232301 (2006).
- [11] A. Lebedev [PHENIX Collaboration], Nucl. Phys. A **854**, 204 (2011);
M. Wysocki [PHENIX Collaboration], Eur. Phys. J. C **62**, 103 (2009).
- [12] M. Gyulassy, I. Vitev and X. N. Wang, Phys. Rev. Lett. **86**, 2537 (2001); X. N. Wang, Phys. Rev. C **63**, 054902 (2001).
- [13] S. Jeon, J. Jalilian-Marian and I. Sarcevic, Nucl. Phys. A **723**, 467 (2003); S. Jeon, J. Jalilian-Marian and I. Sarcevic, Phys. Lett. B **562**, 45 (2003).
- [14] F. Arleo, JHEP **0609**, 015 (2006); F. Arleo, K. J. Eskola, H. Paukkunen and C. A. Salgado, JHEP **1104**, 055 (2011).
- [15] S. Turbide, C. Gale and R. J. Fries, Phys. Rev. Lett. **96**, 032303 (2006);
G. Y. Qin, J. Ruppert, C. Gale, S. Jeon and G. D. Moore, Phys. Rev. C **80**, 054909 (2009);
S. Turbide, C. Gale, E. Frodermann and U. Heinz, Phys. Rev. C **77**, 024909 (2008);
W. Liu and R. J. Fries, Phys. Rev. C **77**, 054902 (2008).
- [16] H. Petersen, arXiv:1105.1766 [nucl-th].
H. Holopainen, H. Niemi and K. J. Eskola, arXiv:1106.4471 [hep-ph].
- [17] J. Auvinen, K. J. Eskola, H. Holopainen and T. Renk, arXiv:1106.4167 [hep-ph].
- [18] M. Gyulassy, P. Levai and I. Vitev, Nucl. Phys. B **571**, 197 (2000); M. Gyulassy, P. Levai and I. Vitev, Phys. Rev. Lett. **85**, 5535 (2000); M. Gyulassy, P. Levai and I. Vitev, Nucl. Phys. B **594**, 371 (2001);
X. f. Guo and X. N. Wang, Phys. Rev. Lett. **85**, 3591 (2000); X. N. Wang and X. f. Guo, Nucl. Phys. A **696**, 788 (2001);
P. B. Arnold, G. D. Moore and L. G. Yaffe, JHEP **0206**, 030 (2002); S. Jeon and G. D. Moore, Phys. Rev. C **71**, 034901 (2005);
C. A. Salgado and U. A. Wiedemann, Phys. Rev. Lett. **89**, 092303 (2002); C. A. Salgado and U. A. Wiedemann, Nucl. Phys. A **715**, 783 (2003); C. A. Salgado and U. A. Wiedemann, Phys. Rev. D **68**, 014008 (2003).
- [19] A. Majumder, J. Phys. G **34**, S377 (2007).
- [20] S. A. Bass, C. Gale, A. Majumder, C. Nonaka, G. Y. Qin, T. Renk, and J. Ruppert, Phys. Rev. C **79**, 024901 (2009).

- [21] T. Renk, Phys. Rev. C **74**, 034906 (2006).
- [22] D. K. Srivastava, J. Phys. G **38**, 055003 (2011).
- [23] X. N. Wang, Z. Huang and I. Sarcevic, Phys. Rev. Lett. **77**, 231 (1996); X. N. Wang and Z. Huang, Phys. Rev. C **55**, 3047 (1997).
- [24] R. Baier, D. Schiff and B. G. Zakharov, Ann. Rev. Nucl. Part. Sci. **50**, 37 (2000); R. Baier, Y. L. Dokshitzer, A. H. Mueller, S. Peigne and D. Schiff, Nucl. Phys. B **484**, 265 (1997); R. Baier, Y. L. Dokshitzer, A. H. Mueller, S. Peigne and D. Schiff, Nucl. Phys. B **483**, 291 (1997); R. Baier, Y. L. Dokshitzer, A. H. Mueller and D. Schiff, Phys. Rev. C **58**, 1706 (1998). See also, D. d'Enterria, arXiv:0902.2011 [nucl-ex]; S. Peigne and A. V. Smilga, Phys. Usp. **52**, 659 (2009) [Usp. Fiz. Nauk **179**, 697 (2009)] [arXiv:0810.5702 [hep-ph]].
- [25] P. Aurenche, M. Fontannaz, J. P. Guillet, B. A. Kniehl and M. Werlen, Eur. Phys. J. C **13**, 347 (2000);
F. Aversa, P. Chiappetta, M. Greco and J. P. Guillet, Nucl. Phys. B **327**, 105 (1989).
- [26] P. Aurenche, M. Fontannaz, J. P. Guillet, B. A. Kniehl, E. Pilon and M. Werlen, Eur. Phys. J. C **9**, 107 (1999);
F. Arleo *et al.*, arXiv:hep-ph/0311131.
- [27] H. L. Lai *et al.*, Phys. Rev. D **55**, 1280 (1997).
- [28] J. Binnewies, B. A. Kniehl and G. Kramer, Phys. Rev. D **52**, 4947 (1995).
- [29] A. Adare *et al.* [PHENIX Collaboration], Phys. Rev. **D76**, 051106 (2007).
- [30] D. de Florian and W. Vogelsang, Phys. Rev. D **71**, 114004 (2005).
- [31] K. J. Eskola, V. J. Kolhinen and C. A. Salgado, Eur. Phys. J. C **9**, 61 (1999);
K. J. Eskola, V. J. Kolhinen and P. V. Ruuskanen, Nucl. Phys. B **535**, 351 (1998).
- [32] A. Adare *et al.* [PHENIX Collaboration], Phys. Rev. Lett. **101**, 232301 (2008).
- [33] A. Adare *et al.* [PHENIX Collaboration], Phys. Rev. Lett. **105**, 142301 (2010).
- [34] A. Adare *et al.* [PHENIX Collaboration], Phys. Rev. Lett. **101**, 162301 (2008).
- [35] B. Schenke, S. Jeon and C. Gale, Phys. Rev. C **83**, 044907 (2011).
- [36] See, e.g., C. Marquet and T. Renk, Phys. Lett. B **685**, 270 (2010); H. Liu, K. Rajagopal and U. A. Wiedemann, Phys. Rev. Lett. **97**, 182301 (2006).
- [37] C. Shen, U. Heinz, P. Huovinen and H. Song, Phys. Rev. C **82**, 054904 (2010);
H. Song, S. A. Bass and U. Heinz, Phys. Rev. C **83**, 054912 (2011);
B. Schenke, S. Jeon and C. Gale, Phys. Rev. Lett. **106**, 042301 (2011).
- [38] B. Müller, Phys. Rev. C **67**, 061901 (2003).
- [39] S. S. Adler *et al.* [PHENIX Collaboration], Phys. Rev. Lett. **98**, 012002 (2007).
- [40] T. Isobe [PHENIX Collaboration], J. Phys. G **34**, S1015 (2007) [arXiv:nucl-ex/0701040].
- [41] R. Chatterjee, E. S. Frodermann, U. W. Heinz and D. K. Srivastava, Phys. Rev. Lett. **96**, 202302 (2006);
R. Chatterjee and D. K. Srivastava, Phys. Rev. C **79**, 021901 (2009).
- [42] A. Adare *et al.* [PHENIX Collaboration], arXiv:1105.4126 [nucl-ex].
- [43] A. M. Hamed, [STAR Collaboration], J. Phys. Conf. Ser. **270**, 012010 (2011) [arXiv:1008.4894 [nucl-ex]].